PROCEEDINGS OF SCIENCE

All-flavor Time-dependent Search for Transient Neutrino Sources

The IceCube Collaboration

(a complete list of authors can be found at the end of the proceedings)

E-mail: jcarpio@icecube.wisc.edu, ali.kheirandish@icecube.wisc.edu, hmniederhausen@icecube.wisc.edu

Transient sources are among the preferred candidates for the sources of high-energy neutrino emission. Intriguing examples so far include blazar flares and tidal disruption events coincident with IceCube neutrinos. Here, we report the first all-flavor, all-sky time-dependent search for neutrino sources by combining IceCube throughgoing tracks, starting tracks and cascades. Throughgoing tracks provide the best sensitivity in the Northern Sky, while cascades have worse angular resolution but yield better sensitivity in the Southern Sky than tracks. The relatively new starting tracks sample has reduced contamination from atmospheric muons. This analysis takes advantage of the strengths of each of the datasets, combining them for increased statistics and obtaining the best accessible all-sky sensitivity for transient searches. In this search, we look for unbound $E^{-\gamma}$ power-law sources, as well as E^{-2} sources with low and high-energy exponential cutoffs, optimizing the sensitivity for the duration of the flares.

Corresponding authors: Jose Carpio[1*], Ali Kheirandish[1], Hans Niederhausen[2]

[1] *University of Nevada Las Vegas*

[2] *Michigan State University*

[*] *Presenter*

39th International Cosmic Ray Conference (ICRC2025)
15–24 July 2025
Geneva, Switzerland

PoS(ICRC2025)1007

1. Introduction

Transient neutrino sources, such as blazar flares, tidal disruption events, and gamma-ray bursts, are among the primary candidates for the origin of high-energy neutrino emission [1]. In 2017, IceCube detected a 290 TeV neutrino spatially coincident with the blazar TXS 0506+056 [2]. Time-integrated searches with 10 years of neutrino tracks showed the transient TXS 0506+056 as the second most significant source in the Northern Sky [3]. However, the neutrino signal is not necessarily accompanied by an electromagnetic counterpart, leaving neutrinos as the only way to observe these sources. These would appear in neutrino data as a clustering of events in the time domain.

Time-dependent searches provide an advantage over the time-integrated ones, for flares that last for $\Delta T \lesssim 100$ days, as it reduces the atmospheric neutrino background, which is relatively uniform in time. Previously, the IceCube collaboration has performed a transient search [4] and multi-flare search [5], but did not find any new significant excesses.

In this study, we aim for improving upon previous searches by utilizing all channels of observations to obtain the best accessible sensitivity for IceCube.

Furthermore, neutrino point source searches have usually looked for generic power-law fluxes $E^{-\gamma}$. However, the expected neutrino flux generally has features beyond a simple power-law. The IceCube collaboration has used alternative parametrizations for the diffuse neutrino flux (see e.g., [6]). More recently, point source searches have also used more sophisticated signal energy spectra, such as Seyfert flux models to search for neutrino emission from Seyfert galaxies [7]. Here, we implement a power-law with low and high-energy cutoffs in the search that could capture the predicted features in prominent transient sources of neutrinos.

2. Method

For the analysis we will use the likelihood (LLH) function $\mathcal{L}$ [8]

$$\ln \mathcal{L} = \sum_i \ln \left[\mathcal{S}_i \frac{n_s}{N} + \left(1 - \frac{n_s}{N}\right) \mathcal{B}_i \right], \tag{1}$$

where $\mathcal{S}_i$ and $\mathcal{B}_i$ are the signal and background probability density functions (pdfs), respectively, for each event i. The signal pdf can be factorized into a spatial pdf term, which describes the spatial clustering of the events around the source, an energy pdf term, describing their energy distribution, and a temporal pdf term, describing the arrival time distribution of the events.

This time-dependent analysis assumes that the temporal pdf follows a Gaussian distribution, centered at T_0 and a standard deviation σ_T. The spatial pdfs are two-dimensional Gaussians, where the reconstructed direction has a standard deviation σ_i. The NT sample was later enhanced by using a Kernel Density Estimate (KDE) so that the spectral shape of the flux is also taken into account, making the spatial pdf more realistic (see e.g., supplemental material in [9] for a description of the KDE method).

The energy pdf is the probability that an event is observed with a given energy at a fixed declination δ and for a given spectral hypothesis. In the case of $E^{-\gamma}$ power-law sources, this introduces an additional parameter, the power-law index γ.

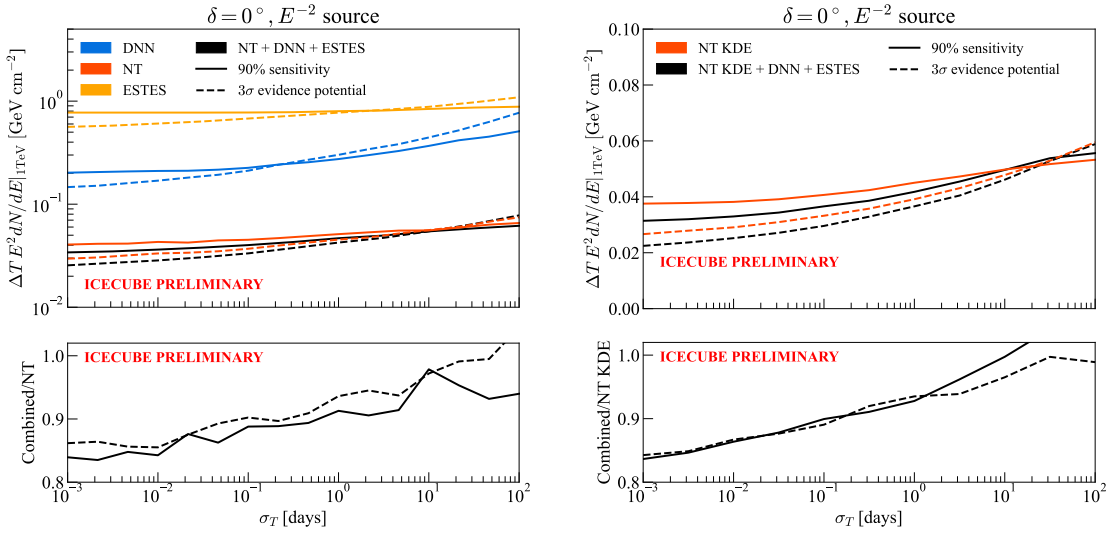

Figure 1: Top left panel: Per-flavor 90% CL sensitivity (solid lines) and 3σ evidence (dashed lines) fluences for an E^{-2} source at declination $\delta = 0°$, for different flare half-widths σ_T and $E^{-\gamma}$ signal flux hypothesis. The blue, red, orange and black lines correspond to DNNCascade, NT, ESTES and combined datasets, respectively. Here, the NT sample assumes Gaussian spatial pdfs. Top right panel: Same as top left panel, but the NT dataset is using KDEs in its spatial and energy pdfs. Bottom left panel: Combined-to-NT fluence ratios. Bottom right panel: Combined-to-NT KDE fluence ratios

Using $\mathcal{L}$, we define the test statistic

$$\mathrm{TS} = 2 \ln \left[\frac{\hat{\sigma}_T}{T_{\mathrm{live}}} \frac{\mathcal{L}(\hat{n}_s, \hat{\gamma}, \hat{T}_0, \hat{\sigma}_T)}{\mathcal{L}(n_s = 0)} \right], \tag{2}$$

where we used the power-law signal hypothesis as an example. $(\hat{n}_s, \hat{\gamma}, \hat{T}_0, \hat{\sigma}_T)$ is the parameter set that maximizes the term in square brackets. T_{live} is the livetime of the dataset. The term $/\sigma_T/T_{\mathrm{live}}$ is a factor that penalizes short bursts due to their large trial factors (see e.g., [8]). In our analysis, we restrict the parameters to $n_s \geq 0, \gamma \in [1, 4]$ (for power-law fits) , $\sigma_T \in [0, \sigma_{T,\mathrm{max}}]$, where $\sigma_{T,\mathrm{max}}$ is half the livetime of the dataset. For the combined dataset, we define $\sigma_{T,\mathrm{max}}$ as half the longest livetime between the datasets.

With the TS defined, we create the background and signal TS distributions by running trials. The background events within a trial are obtained from scrambled data, whereas the signal events are obtained from simulations. We define the 90% CL sensitivity as the signal flux required for the signal TS to be larger than the background median 90% of the time. Additionally, we define the 3σ evidence potential as the injected flux required for the probability of the signal TS to have a $p-$value $p < 2.7 \times 10^{-3}$ (the 3σ threshold) is equal to 50%. The evidence potential at other significances is defined in a similar fashion, by modifying the $p-$value threshold to the corresponding number of σ.

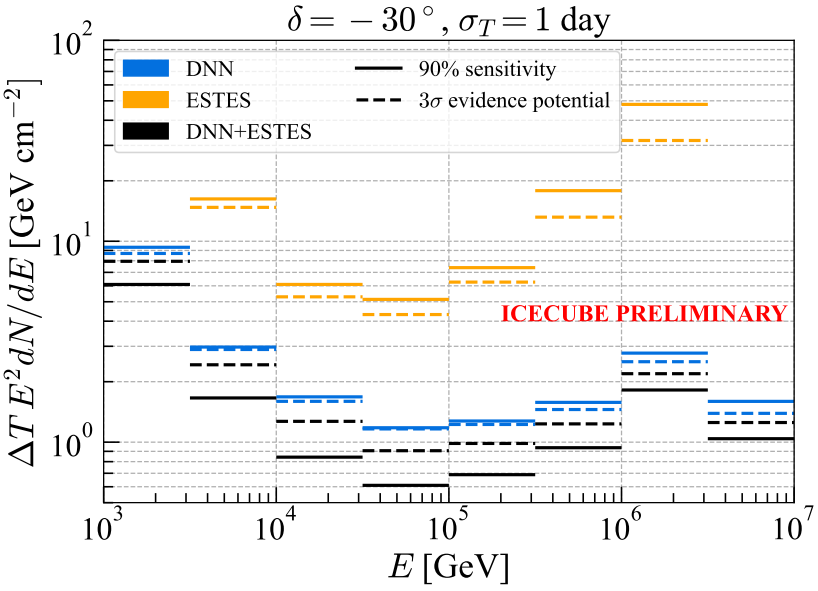

Figure 2: Per-flavor 90% CL sensitivity (solid lines) and 3σ evidence potential (dashed lines) fluences to a neutrino flare of half-width σ_T. The blue, orange and black lines correspond to DNNCascade, ESTES and combined datasets, respectively.

3. Analysis performance

3.1 Power-law fits

In this section, our signal hypothesis to calculate TS will be a point source with an $E^{-\gamma}$ power-law spectrum, where $\gamma \in [1, 4]$, where the fit parameters are n_s, γ, T_0 and σ_T.

We show in Figure 1 the E^{-2} sensitivity and evidence potential for different flare half-widths σ_T, for a source at the horizon. Here we assume $E^{-\gamma}$ signal fluxes, as is typically used in point source searches. We are reporting fluence (time-integrated fluxes) as $\Delta T dN/dE$, evaluated at 1 TeV. The left panels show the sensitivity of the DNNCascade, NT and ESTES samples. Here, the NT data is assuming Gaussian spatial pdfs, not KDEs. The most notable feature is that the sensitivity worsens for longer-duration flares. For flares shorter than $\sim$ 0.1 days, the sensitivity flattens, because we are approaching the background-free regime. Flares longer than 10 days have more background contamination, degrading the sensitivity. We see that the NT sample provides the best sensitivity at the horizon among the three datasets, as it has the largest statistics and its good angular resolution improves the spatial pdfs for signal events. By combining the datasets, we see a 10% – 15% improvement in sensitivity and evidence potential, but the improvement is less significant for flares longer than $\sim$ 1 day. In the right panels of Figure 1, the NT sample uses KDEs in its signal pdf. This change gives a minor improvement in the sensitivity for flares shorter than a day. We see that the 3σ evidence potential is at a lower flux than the sensitivity for short flares, and the two curves cross between 0.1 and 1 day, depending on the sample. Changing the TS threshold criteria will move the location of the crossing point and is thus dependent on the definition

of sensitivity and evidence.

We calculate the differential sensitivity and 3σ evidence potential for a flare with $\sigma_T = 1$ day at a declination $\delta = -30°$. We did this by dividing the energy range into two bins per energy decade, then injected neutrinos at each bin assuming an E^{-2} spectrum. The result is shown in Figure 2. We see that both the differential sensitivity and 3σ evidence is best at $E \sim 100$ TeV. Within this energy range, the background event rate is low. As we go to higher energies, we see that the sensitivity worsens. The improvement on the last energy bin is due to the Glashow resonance for cascade events, where the $\bar{\nu}_e$ charged-current interaction cross section is enhanced. The combined analysis also provides a good improvement when compared to the NT samples alone.

3.2 Two-sided cutoff fits

In this section, we introduce an additional energy pdf for the signal hypothesis: an E^{-2} flux with two energy cutoffs of the form

$$e^{-E_L/E} E^{-2} e^{-E/E_H}, \tag{3}$$

where E_L and E_H are the low and high-energy cutoffs, respectively. We will also refer to this flux as a two-sided cutoff. The inclusion of E_H is motivated by the presence of a maximum cosmic ray energy, while E_L accounts for the minimum proton energy required to initiate $p\gamma$ or pp interactions in the source and lead to neutrino production. The use of a more representative signal hypothesis allows for a more accurate sensitivity. Based on the differential sensitivities, having a two-sided cutoff flux that peaks around 100 TeV could potentially be missed in a power-law fit.

With this new flux hypothesis, the power-law index $\gamma = 2$ is fixed when calculating TS. We restrict $E_L \in [100\ \text{GeV}, 10\ \text{TeV}]$ and $E_H \in [10\ \text{TeV}, 100\ \text{PeV}]$. When fitting for two-sided cutoffs, the fit parameters are n_s, E_L, E_H, T_0 and σ_T.

We proceed to compare the performance between flux hypotheses. We assume that the true signal flux is given by Eq. (3), with $E_L = 1$ TeV , $E_H = 100$ TeV. We then compare the 3σ evidence potential for this injected flux under a two-sided cutoff and a power-law hypothesis separately. First, we identify the 3σ evidence potential for the two-sided cutoff hypothesis. We then inject this 3σ two-sided cutoff flux, as the true signal flux, and perform a power-law fit instead. Note that by swapping to a different signal hypothesis, the signal pdfs going into equation (2) have changed, and thus the TS adopts a different value even if the events in a given trial are the same. Hence, we have to create new signal and background TS distributions. In a power-law fit, the trials for the injected 3σ two-sided cutoff flux will no longer generate a TS which is 50% of the time above the 3σ threshold of the new background TS distribution (i.e. it is not a 3σ flux under this new hypothesis). Under the power-law hypothesis, we can compute the new number of sigma associated with this two-sided cutoff flux, which we call the recovered significance. In this sense, we say that the 3σ two-sided cutoff flux has been *recovered* with a different significance.

We show the significance recovery in Figure 3. For this example, the left (right) panel uses the DNNCascade (NT) sample only. The NT sample in the right panel does not use KDEs. We find that a two-sided cutoff flux is not recovered at the 3σ level in power-law searches. In fact, we only recover it at 1σ for the shortest time windows. As the flare duration increases, the recovery improves. We found that the TS distribution is not significantly different between signal hypotheses.

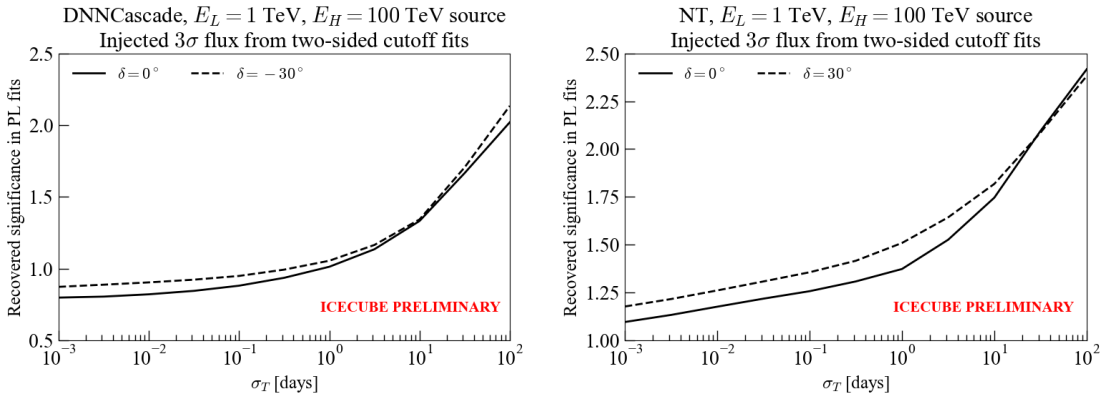

Figure 3: Recovered significance in power-law fits after injecting the 3σ evidence flux for two-sided cutoffs, for different flare half-widths σ_T. Left (right) panel corresponds to the DNNCascade (NT) sample.

Hence, the loss in significance is mostly tied to the reconstruction of the signal pdf parameters. The power-law hypothesis tends to fit for $\gamma > 2$, which causes an overfitting of the signal parameter n_s. In the case of flares with $\sigma_T \lesssim 1$ day, the injection of a 3σ two-sided cutoff flux amounts to injecting $\approx 3-4$ signal events. For these values of σ_T, the injected number of events is too low for the LLH to fully take advantage of the background-free regime and reduce the n_s bias.

4. Conclusions

This is the first multi-flavor time-dependent all-sky point source search. Here we covered the difference in performance between datasets and its improvement upon combining them. We report a $\approx 15\%$ improvement in sensitivity and evidence potential for E^{-2} sources at the horizon, when using the combined dataset. We also find that a power-law fit in our LLH analysis might miss a two-sided cutoff signal, particularly for flares with $\sigma_T \lesssim 1$ day.

References

[1] K. Murase and I. Bartos, *Ann. Rev. Nucl. Part. Sci.* **69** (2019) 477–506.

[2] **IceCube** Collaboration, M. G. Aartsen *et al.*, *Science* **361** no. 6398, (2018) 147–151.

[3] **IceCube** Collaboration, M. G. Aartsen *et al.*, *Phys. Rev. Lett.* **124** no. 5, (2020) 051103.

[4] **IceCube** Collaboration, R. Abbasi *et al.*, *Astrophys. J.* **967** no. 1, (2024) 48.

[5] **IceCube** Collaboration, R. Abbasi *et al.*, *Astrophys. J. Lett.* **920** no. 2, (2021) L45.

[6] **IceCube** Collaboration, R. Naab, E. Ganster, and Z. Zhang, "Measurement of the astrophysical diffuse neutrino flux in a combined fit of IceCube's high energy neutrino data," in *38th International Cosmic Ray Conference*. 7, 2023. arXiv:2308.00191 [astro-ph.HE].

[7] **IceCube** Collaboration, R. Abbasi *et al.* https://arxiv.org/abs/2406.07601.

[8] J. Braun, M. Baker, J. Dumm, C. Finley, A. Karle, and T. Montaruli, *Astropart. Phys.* **33** (2010) 175–181.

[9] **IceCube** Collaboration, R. Abbasi *et al.*, *Science* **378** no. 6619, (2022) 538–543.

Full Author List: IceCube Collaboration

R. Abbasi[16], M. Ackermann[63], J. Adams[17], S. K. Agarwalla[39, a], J. A. Aguilar[10], M. Ahlers[21], J.M. Alameddine[22], S. Ali[35], N. M. Amin[43], K. Andeen[41], C. Argüelles[13], Y. Ashida[52], S. Athanasiadou[63], S. N. Axani[43], R. Babu[23], X. Bai[49], J. Baines-Holmes[39], A. Balagopal V.[39, 43], S. W. Barwick[29], S. Bash[26], V. Basu[52], R. Bay[6], J. J. Beatty[19, 20], J. Becker Tjus[9, b], P. Behrens[1], J. Beise[61], C. Bellenghi[26], B. Benkel[63], S. BenZvi[51], D. Berley[18], E. Bernardini[47, c], D. Z. Besson[35], E. Blaufuss[18], L. Bloom[58], S. Blot[63], I. Bodo[39], F. Bontempo[30], J. Y. Book Motzkin[13], C. Boscolo Meneguolo[47, c], S. Böser[40], O. Botner[61], J. Böttcher[1], J. Braun[39], B. Brinson[4], Z. Brisson-Tsavoussis[32], R. T. Burley[2], D. Butterfield[39], M. A. Campana[48], K. Carloni[13], J. Carpio[33, 34], S. Chattopadhyay[39, a], N. Chau[10], Z. Chen[55], D. Chirkin[39], S. Choi[52], B. A. Clark[18], A. Coleman[61], P. Coleman[1], G. H. Collin[14], D. A. Coloma Borja[47], A. Connolly[19, 20], J. M. Conrad[14], R. Corley[52], D. F. Cowen[59, 60], C. De Clercq[11], J. J. DeLaunay[59], D. Delgado[13], T. Delmeulle[10], S. Deng[1], P. Desiati[39], K. D. de Vries[11], G. de Wasseige[36], T. DeYoung[23], J. C. Díaz-Vélez[39], S. DiKerby[23], M. Dittmer[42], A. Domi[25], L. Draper[52], L. Dueser[1], D. Durnford[24], K. Dutta[40], M. A. DuVernois[39], T. Ehrhardt[40], L. Eidenschink[26], A. Eimer[25], P. Eller[26], E. Ellinger[62], D. Elsässer[22], R. Engel[30, 31], H. Erpenbeck[39], W. Esmail[42], S. Eulig[13], J. Evans[18], P. A. Evenson[43], K. L. Fan[18], K. Fang[39], K. Farrag[15], A. R. Fazely[5], A. Fedynitch[57], N. Feigl[8], C. Finley[54], L. Fischer[63], D. Fox[59], A. Franckowiak[9], S. Fukami[63], P. Fürst[1], J. Gallagher[38], E. Ganster[1], A. Garcia[13], M. Garcia[43], G. Garg[39, a], E. Genton[13, 36], L. Gerhardt[7], A. Ghadimi[58], C. Glaser[61], T. Glüsenkamp[61], J. G. Gonzalez[43], S. Goswami[33, 34], A. Granados[23], D. Grant[12], S. J. Gray[18], S. Griffin[39], S. Griswold[51], K. M. Groth[21], D. Guevel[39], C. Günther[1], P. Gutjahr[22], C. Ha[53], C. Haack[25], A. Hallgren[61], L. Halve[1], F. Halzen[39], L. Hamacher[1], M. Ha Minh[26], M. Handt[1], K. Hanson[39], J. Hardin[14], A. A. Harnisch[23], P. Hatch[32], A. Haungs[30], J. Häußler[1], K. Helbing[62], J. Hellrung[9], B. Henke[23], L. Hennig[25], F. Henningsen[12], L. Heuermann[1], R. Hewett[17], N. Heyer[61], S. Hickford[62], A. Hidvegi[54], C. Hill[15], G. C. Hill[2], R. Hmaid[15], K. D. Hoffman[18], D. Hooper[39], S. Hori[39], K. Hoshina[39, d], M. Hostert[13], W. Hou[30], T. Huber[30], K. Hultqvist[54], K. Hymon[22, 57], A. Ishihara[15], W. Iwakiri[15], M. Jacquart[21], S. Jain[39], O. Janik[25], M. Jansson[36], M. Jeong[52], M. Jin[13], N. Kamp[13], D. Kang[30], W. Kang[48], X. Kang[48], A. Kappes[42], L. Kardum[22], T. Karg[63], M. Karl[26], A. Karle[39], A. Katil[24], M. Kauer[39], J. L. Kelley[39], M. Khanal[52], A. Khatee Zathul[39], A. Kheirandish[33, 34], H. Kimku[53], J. Kiryluk[55], C. Klein[25], S. R. Klein[6, 7], Y. Kobayashi[15], A. Kochocki[23], R. Koirala[43], H. Kolanoski[8], T. Kontrimas[26], L. Köpke[40], C. Kopper[25], D. J. Koskinen[21], P. Koundal[43], M. Kowalski[8, 63], T. Kozynets[21], N. Krieger[9], J. Krishnamoorthi[39, a], T. Krishnan[13], K. Kruiswijk[36], E. Krupczak[23], A. Kumar[63], E. Kun[9], N. Kurahashi[48], N. Lad[63], C. Lagunas Gualda[26], L. Lallement Arnaud[10], M. Lamoureux[36], M. J. Larson[18], F. Lauber[62], J. P. Lazar[36], K. Leonard DeHolton[60], A. Leszczyńska[43], J. Liao[4], C. Lin[43], Y. T. Liu[60], M. Liubarska[24], C. Love[48], L. Lu[39], F. Lucarelli[27], W. Luszczak[19, 20], Y. Lyu[6, 7], J. Madsen[39], E. Magnus[11], K. B. M. Mahn[23], Y. Makino[39], E. Manao[26], S. Mancina[47, e], A. Mand[39], I. C. Mariş[10], S. Marka[45], Z. Marka[45], L. Marten[1], I. Martinez-Soler[13], R. Maruyama[44], J. Mauro[36], F. Mayhew[23], F. McNally[37], J. V. Mead[21], K. Meagher[39], S. Mechbal[63], A. Medina[20], M. Meier[15], Y. Merckx[11], L. Merten[9], J. Mitchell[5], L. Molchany[49], T. Montaruli[27], R. W. Moore[24], Y. Morii[15], A. Mosbrugger[25], M. Moulai[39], D. Mousadi[63], E. Moyaux[36], T. Mukherjee[30], R. Naab[63], M. Nakos[39], U. Naumann[62], J. Necker[63], L. Neste[54], M. Neumann[42], H. Niederhausen[23], M. U. Nisa[23], K. Noda[15], A. Noell[1], A. Novikov[43], A. Obertacke Pollmann[15], V. O'Dell[39], A. Olivas[18], R. Orsoe[26], J. Osborn[39], E. O'Sullivan[61], V. Palusova[40], H. Pandya[43], A. Parenti[10], N. Park[32], V. Parrish[23], E. N. Paudel[58], L. Paul[49], C. Pérez de los Heros[61], T. Pernice[63], J. Peterson[39], M. Plum[49], A. Pontén[61], V. Poojyam[58], Y. Popovych[40], M. Prado Rodriguez[39], B. Pries[23], R. Procter-Murphy[18], G. T. Przybylski[7], L. Pyras[52], C. Raab[36], J. Rack-Helleis[40], N. Rad[63], M. Ravn[61], K. Rawlins[3], Z. Rechav[39], A. Rehman[43], I. Reistroffer[49], E. Resconi[26], S. Reusch[63], C. D. Rho[56], W. Rhode[22], L. Ricca[36], B. Riedel[39], A. Rifaie[62], E. J. Roberts[2], S. Robertson[6, 7], M. Rongen[25], A. Rosted[15], C. Rott[52], T. Ruhe[22], L. Ruohan[26], D. Ryckbosch[28], J. Saffer[31], D. Salazar-Gallegos[23], P. Sampathkumar[30], A. Sandrock[62], G. Sanger-Johnson[23], M. Santander[58], S. Sarkar[46], J. Savelberg[1], M. Scarnera[36], P. Schaile[26], M. Schaufel[1], H. Schieler[30], S. Schindler[25], L. Schlickmann[40], B. Schlüter[42], F. Schlüter[10], N. Schmeisser[62], T. Schmidt[18], F. G. Schröder[30, 43], L. Schumacher[25], S. Schwirn[1], S. Sclafani[18], D. Seckel[43], L. Seen[39], M. Seikh[35], S. Seunarine[50], P. A. Sevle Myhr[36], R. Shah[48], S. Shefali[31], N. Shimizu[15], B. Skrzypek[6], R. Snihur[39], J. Soedingrekso[22], A. Søgaard[21], D. Soldin[52], P. Soldin[1], G. Sommani[9], C. Spannfellner[26], G. M. Spiczak[50], C. Spiering[63], J. Stachurska[28], M. Stamatikos[20], T. Stanev[43], T. Stezelberger[7], T. Stürwald[62], T. Stuttard[21], G. W. Sullivan[18], I. Taboada[4], S. Ter-Antonyan[5], A. Terliuk[26], A. Thakuri[49], M. Thiesmeyer[39], W. G. Thompson[13], J. Thwaites[39], S. Tilav[43], K. Tollefson[23], S. Toscano[10], D. Tosi[39], A. Trettin[63], A. K. Upadhyay[39, a], K. Upshaw[5], A. Vaidyanathan[41], N. Valtonen-Mattila[9, 61], J. Valverde[41], J. Vandenbroucke[39], T. van Eeden[63], N. van Eijndhoven[11], L. van Rootselaar[22], J. van Santen[63], F. J. Vara Carbonell[42], F. Varsi[31], M. Venugopal[30], M. Vereecken[36], S. Vergara Carrasco[17], S. Verpoest[43], D. Veske[45], A. Vijai[18], J. Villarreal[14], C. Walck[54], A. Wang[4], E. Warrick[58], C. Weaver[23], P. Weigel[14], A. Weindl[30], J. Weldert[40], A. Y. Wen[13], C. Wendt[39], J. Werthebach[22], M. Weyrauch[30], N. Whitehorn[23], C. H. Wiebusch[1], D. R. Williams[58], L. Witthaus[22], M. Wolf[26], G. Wrede[25], X. W. Xu[5], J. P. Yañez[24], Y. Yao[39], E. Yildizci[39], S. Yoshida[15], R. Young[35], F. Yu[13], S. Yu[52], T. Yuan[39], A. Zegarelli[9], S. Zhang[23], Z. Zhang[55], P. Zhelnin[13], P. Zilberman[39]

[1] III. Physikalisches Institut, RWTH Aachen University, D-52056 Aachen, Germany
[2] Department of Physics, University of Adelaide, Adelaide, 5005, Australia
[3] Dept. of Physics and Astronomy, University of Alaska Anchorage, 3211 Providence Dr., Anchorage, AK 99508, USA
[4] School of Physics and Center for Relativistic Astrophysics, Georgia Institute of Technology, Atlanta, GA 30332, USA
[5] Dept. of Physics, Southern University, Baton Rouge, LA 70813, USA
[6] Dept. of Physics, University of California, Berkeley, CA 94720, USA
[7] Lawrence Berkeley National Laboratory, Berkeley, CA 94720, USA
[8] Institut für Physik, Humboldt-Universität zu Berlin, D-12489 Berlin, Germany
[9] Fakultät für Physik & Astronomie, Ruhr-Universität Bochum, D-44780 Bochum, Germany
[10] Université Libre de Bruxelles, Science Faculty CP230, B-1050 Brussels, Belgium

[11] Vrije Universiteit Brussel (VUB), Dienst ELEM, B-1050 Brussels, Belgium
[12] Dept. of Physics, Simon Fraser University, Burnaby, BC V5A 1S6, Canada
[13] Department of Physics and Laboratory for Particle Physics and Cosmology, Harvard University, Cambridge, MA 02138, USA
[14] Dept. of Physics, Massachusetts Institute of Technology, Cambridge, MA 02139, USA
[15] Dept. of Physics and The International Center for Hadron Astrophysics, Chiba University, Chiba 263-8522, Japan
[16] Department of Physics, Loyola University Chicago, Chicago, IL 60660, USA
[17] Dept. of Physics and Astronomy, University of Canterbury, Private Bag 4800, Christchurch, New Zealand
[18] Dept. of Physics, University of Maryland, College Park, MD 20742, USA
[19] Dept. of Astronomy, Ohio State University, Columbus, OH 43210, USA
[20] Dept. of Physics and Center for Cosmology and Astro-Particle Physics, Ohio State University, Columbus, OH 43210, USA
[21] Niels Bohr Institute, University of Copenhagen, DK-2100 Copenhagen, Denmark
[22] Dept. of Physics, TU Dortmund University, D-44221 Dortmund, Germany
[23] Dept. of Physics and Astronomy, Michigan State University, East Lansing, MI 48824, USA
[24] Dept. of Physics, University of Alberta, Edmonton, Alberta, T6G 2E1, Canada
[25] Erlangen Centre for Astroparticle Physics, Friedrich-Alexander-Universität Erlangen-Nürnberg, D-91058 Erlangen, Germany
[26] Physik-department, Technische Universität München, D-85748 Garching, Germany
[27] Département de physique nucléaire et corpusculaire, Université de Genève, CH-1211 Genève, Switzerland
[28] Dept. of Physics and Astronomy, University of Gent, B-9000 Gent, Belgium
[29] Dept. of Physics and Astronomy, University of California, Irvine, CA 92697, USA
[30] Karlsruhe Institute of Technology, Institute for Astroparticle Physics, D-76021 Karlsruhe, Germany
[31] Karlsruhe Institute of Technology, Institute of Experimental Particle Physics, D-76021 Karlsruhe, Germany
[32] Dept. of Physics, Engineering Physics, and Astronomy, Queen's University, Kingston, ON K7L 3N6, Canada
[33] Department of Physics & Astronomy, University of Nevada, Las Vegas, NV 89154, USA
[34] Nevada Center for Astrophysics, University of Nevada, Las Vegas, NV 89154, USA
[35] Dept. of Physics and Astronomy, University of Kansas, Lawrence, KS 66045, USA
[36] Centre for Cosmology, Particle Physics and Phenomenology - CP3, Université catholique de Louvain, Louvain-la-Neuve, Belgium
[37] Department of Physics, Mercer University, Macon, GA 31207-0001, USA
[38] Dept. of Astronomy, University of Wisconsin—Madison, Madison, WI 53706, USA
[39] Dept. of Physics and Wisconsin IceCube Particle Astrophysics Center, University of Wisconsin—Madison, Madison, WI 53706, USA
[40] Institute of Physics, University of Mainz, Staudinger Weg 7, D-55099 Mainz, Germany
[41] Department of Physics, Marquette University, Milwaukee, WI 53201, USA
[42] Institut für Kernphysik, Universität Münster, D-48149 Münster, Germany
[43] Bartol Research Institute and Dept. of Physics and Astronomy, University of Delaware, Newark, DE 19716, USA
[44] Dept. of Physics, Yale University, New Haven, CT 06520, USA
[45] Columbia Astrophysics and Nevis Laboratories, Columbia University, New York, NY 10027, USA
[46] Dept. of Physics, University of Oxford, Parks Road, Oxford OX1 3PU, United Kingdom
[47] Dipartimento di Fisica e Astronomia Galileo Galilei, Università Degli Studi di Padova, I-35122 Padova PD, Italy
[48] Dept. of Physics, Drexel University, 3141 Chestnut Street, Philadelphia, PA 19104, USA
[49] Physics Department, South Dakota School of Mines and Technology, Rapid City, SD 57701, USA
[50] Dept. of Physics, University of Wisconsin, River Falls, WI 54022, USA
[51] Dept. of Physics and Astronomy, University of Rochester, Rochester, NY 14627, USA
[52] Department of Physics and Astronomy, University of Utah, Salt Lake City, UT 84112, USA
[53] Dept. of Physics, Chung-Ang University, Seoul 06974, Republic of Korea
[54] Oskar Klein Centre and Dept. of Physics, Stockholm University, SE-10691 Stockholm, Sweden
[55] Dept. of Physics and Astronomy, Stony Brook University, Stony Brook, NY 11794-3800, USA
[56] Dept. of Physics, Sungkyunkwan University, Suwon 16419, Republic of Korea
[57] Institute of Physics, Academia Sinica, Taipei, 11529, Taiwan
[58] Dept. of Physics and Astronomy, University of Alabama, Tuscaloosa, AL 35487, USA
[59] Dept. of Astronomy and Astrophysics, Pennsylvania State University, University Park, PA 16802, USA
[60] Dept. of Physics, Pennsylvania State University, University Park, PA 16802, USA
[61] Dept. of Physics and Astronomy, Uppsala University, Box 516, SE-75120 Uppsala, Sweden
[62] Dept. of Physics, University of Wuppertal, D-42119 Wuppertal, Germany
[63] Deutsches Elektronen-Synchrotron DESY, Platanenallee 6, D-15738 Zeuthen, Germany
[a] also at Institute of Physics, Sachivalaya Marg, Sainik School Post, Bhubaneswar 751005, India
[b] also at Department of Space, Earth and Environment, Chalmers University of Technology, 412 96 Gothenburg, Sweden
[c] also at INFN Padova, I-35131 Padova, Italy
[d] also at Earthquake Research Institute, University of Tokyo, Bunkyo, Tokyo 113-0032, Japan
[e] now at INFN Padova, I-35131 Padova, Italy

PoS(ICRC2025)1007

Acknowledgments

The authors gratefully acknowledge the support from the following agencies and institutions: USA – U.S. National Science Foundation-Office of Polar Programs, U.S. National Science Foundation-Physics Division, U.S. National Science Foundation-EPSCoR, U.S. National Science Foundation-Office of Advanced Cyberinfrastructure, Wisconsin Alumni Research Foundation, Center for High Throughput Computing (CHTC) at the University of Wisconsin–Madison, Open Science Grid (OSG), Partnership to Advance Throughput Computing (PATh), Advanced Cyberinfrastructure Coordination Ecosystem: Services & Support (ACCESS), Frontera and Ranch computing project at the Texas Advanced Computing Center, U.S. Department of Energy-National Energy Research Scientific Computing Center, Particle astrophysics research computing center at the University of Maryland, Institute for Cyber-Enabled Research at Michigan State University, Astroparticle physics computational facility at Marquette University, NVIDIA Corporation, and Google Cloud Platform; Belgium – Funds for Scientific Research (FRS-FNRS and FWO), FWO Odysseus and Big Science programmes, and Belgian Federal Science Policy Office (Belspo); Germany – Bundesministerium für Forschung, Technologie und Raumfahrt (BMFTR), Deutsche Forschungsgemeinschaft (DFG), Helmholtz Alliance for Astroparticle Physics (HAP), Initiative and Networking Fund of the Helmholtz Association, Deutsches Elektronen Synchrotron (DESY), and High Performance Computing cluster of the RWTH Aachen; Sweden – Swedish Research Council, Swedish Polar Research Secretariat, Swedish National Infrastructure for Computing (SNIC), and Knut and Alice Wallenberg Foundation; European Union – EGI Advanced Computing for research; Australia – Australian Research Council; Canada – Natural Sciences and Engineering Research Council of Canada, Calcul Québec, Compute Ontario, Canada Foundation for Innovation, WestGrid, and Digital Research Alliance of Canada; Denmark – Villum Fonden, Carlsberg Foundation, and European Commission; New Zealand – Marsden Fund; Japan – Japan Society for Promotion of Science (JSPS) and Institute for Global Prominent Research (IGPR) of Chiba University; Korea – National Research Foundation of Korea (NRF); Switzerland – Swiss National Science Foundation (SNSF).